

# Revealing the Nature of Dark Energy Using Bayesian Evidence

T. D. Saini, J. Weller and S. L. Bridle

*Institute of Astronomy, University of Cambridge, Madingley Road, Cambridge CB3 0HA.*

In original form 9 November 2018

## ABSTRACT

We apply the Bayesian concept of ‘evidence’ to reveal systematically the nature of dark energy from present and future supernova luminosity distance measurements. We express the unknown dark energy equation of state  $w(z)$  as a low order polynomial in redshift and use evidence to find the polynomial order, thereby establishing the minimum order required by the data. We apply this method to the current supernova data, and with a prior  $-1 \leq w(z) \leq 1$  and  $\Omega_m = 0.3 \pm 0.05$ , obtain a large probability of 91% for the cosmological constant model, with the remaining 9% assigned to the two more complex models tested. We also investigate the use of evidence for future supernova data sets such as distances obtainable from surveys like the Supernova Acceleration Probe (SNAP). Given a low uncertainty on the present day matter density we find that, if the underlying dark energy model is only modestly evolving, then a constant  $w(z)$  fit is sufficient. However, if the evolution of the dark energy equation of state to linear order is larger than  $|w_1| \gtrsim 0.5$ , then the evolution can be established with statistical significance. For models where we can assume the prior  $-1 \leq w(z) \leq 1$ , the correct polynomial order can be established even for modestly evolving equations of state.

**Key words:** cosmology:theory – methods: statistical –cosmological parameters.

## 1 INTRODUCTION

Observations of distant supernovae give strong indications that the expansion of the universe is accelerating (Riess et al. 1998; Perlmutter et al. 1999; Riess et al. 2001; Tonry et al. 2003). Indications for a low matter density universe are provided by X-ray observations of rich clusters (Bahcall & Fan 1998; Mohr, Mathiesen & Evrard 1999; Dodelson & Knox 2000), which recently has been confirmed with remarkable accuracy (Allen, Schmidt & Fabian 2002). If cosmic microwave background (CMB) observations (Hinshaw et al. 2003) are combined with large scale structure surveys, such as the two degree Field Galaxy Redshift Survey (2dFGRS) (Percival et al. 2002), the best fit cosmological model is a flat FRW universe with  $\Omega_\Lambda \sim 0.7$  and  $\Omega_m \sim 0.3$  (Spergel et al. 2003).

In the simplest case these observations are explained by the addition of a cosmological constant term in the Einstein’s theory of gravity. The cosmological constant is often identified with the energy density of the vacuum (Zel’dovich 1968), but explaining its small value today ( $10^{-120} M_{\text{Pl}}^4$ ) in terms of fundamental physics has remained unsuccessful (Weinberg 1989; Carroll 2001). Therefore, attempts have been made to explain the missing dark energy

as the energy density of a minimally coupled scalar field called Quintessence.

Due to the slow roll of the Quintessence field (Wetterich 1988; Peebles & Ratra 1988; Ratra & Peebles 1988) the universe can become dominated by vacuum energy and the expansion begins to accelerate. In these models the energy in the scalar field becomes important only at relatively late times, giving ample time for the growth of structures in the universe; while tracker like solutions for the field help towards ameliorating the fine tuning problem faced by a pure cosmological constant (Steinhardt, Wang & Zlatev 1999).

At present there are a large number of models that can describe the observed acceleration in the expansion of the universe. These models differ from a cosmological constant mainly through their equation of state  $p_Q = w\rho_Q$ . By assuming a constant equation of state the current bounds are  $w \lesssim -(0.6 - 0.8)$  (Spergel et al. 2003). Although most models predict  $w \geq -1$ , this is not necessary in non-minimally coupled field models (Uzan 1999; Chiba 1999; Amendola 2000) or models with a non-canonical kinetic term (Armendariz-Picon, Mukhanov & Steinhardt 2000).

One of the most promising probes for dark energy are future supernova observations, such as the proposed Su-

arXiv:astro-ph/0305526v1 28 May 2003

pernova Acceleration Probe - SNAP<sup>1</sup> (Aldering et al. 2002), the w project ESSENCE<sup>2</sup> (Garnavich et al. 2003) and the Canada - France - Hawaii Telescope Legacy Survey (CFHTLS)<sup>3</sup>. The potential of a SNAP class experiment in distinguishing theoretical models has been investigated in great detail in various works.

Most methods approximate the dark energy equation of state  $w(z)$  in terms of low order polynomials, or other simple fitting functions (Efstathiou 1999; Maor, Brustein & Steinhardt 2001; Goliath 2001; Weller & Albrecht 2001; Weller & Albrecht 2002; Gerke & Efstathiou 2002). A polynomial approximation is easily interpreted in terms of weighted means of the true equation of state (Saini et al. 2003). The polynomial approximation naturally allows us to phrase three interesting questions about the dark energy: First is our universe described by a cosmological constant ( $w = -1$ ), second is the equation of state a constant and  $w \neq -1$ ? and third, the most general case, is  $w$  evolving with redshift? To answer these questions we need to decide on the basis of data which polynomial order is required to fit the data *adequately*, regardless of the fitted values of the parameters. The fact that polynomial coefficients are related in a simple way to the true equation of state also allows asking further questions regarding the possible time evolution of dark energy.

The Bayesian construct ‘evidence’ answers precisely this type of question. The method has the usual likelihood ratio test built into it, as well as the sensible criterion for penalising models with a large number of parameters, known as the Occam’s razor term (MacKay 1991; Sivia 1996). Our main aim in this paper is to use this concept to formulate the dark energy problem as a model selection problem, and to quantify the requirements of the present and the future data for elaborate modelling. In addition the method is easily extended to differentiate between the diverse theoretical models for quintessence, even when their parameterizations are totally unrelated.

In Section 2 we introduce the concept of evidence and illustrate its meaning using a simple example. Section 3 contains a brief overview of Type Ia supernovae as standard candles, and a brief description of the SNAP mission. In Section 4 we use evidence to calculate the acceptance probability for simple models of dark energy by using the currently available SNe data. We investigate the future prospects for discriminating amongst various dark energy models by simulating SNAP like data and applying the evidence procedure. Furthermore we analyse how prior information on the matter density and the dark energy parameters is affecting evidence. Our conclusions are presented in Section 5.

## 2 BAYESIAN MODEL SELECTION: EVIDENCE

The notion of *evidence* is not frequently used in the astronomical literature, therefore we review the Bayesian method

for model selection, and then apply it to the problem of inferring the polynomial order required by a given data set. For further details see Sivia (1996).

### 2.1 Mathematical framework

A model consists of a set of rules to predict data from a given set of parameters and a *prior* which quantifies the probabilities of the different parameter values in the absence of any data. Consider a set of models (hypotheses)  $\{H\}$ . From Bayes’ theorem the probability that  $H$  is true is

$$P(H|D) = \frac{P(D|H)P(H)}{P(D)}, \quad (1)$$

where  $D$  denotes the observed data. This shows how our prior probability  $P(H)$  is modified by the presence of the data to give the *posterior* probability  $P(H|D)$ .

The probability  $P(D|H)$  is the probability of data marginalized over the parameter values in the model  $H$ . This can be seen more clearly from the following. Writing the parameters for model  $H$  as  $\theta$ , Bayes’ theorem gives for the posterior probability of the parameters given the data and model:

$$P(\theta|D, H) = \frac{P(D|\theta, H)P(\theta|H)}{P(D|H)}. \quad (2)$$

$P(D|\theta, H)$  is the usual likelihood of data, given the model and its parameters, and  $P(\theta|H)$  are the priors on the parameters. The required quantity is the denominator in the right hand side which is found from normalizing the left hand side to unity to be

$$\mathcal{E} \equiv P(D|H) = \int d^n \theta P(D|\theta, H)P(\theta|H), \quad (3)$$

where  $\mathcal{E}$  denotes the evidence of the hypothesis  $H$ .

If the data is predicted by a large volume of the parameter space allowed by the priors then the model gets a high probability (evidence), which is a very desirable feature. The denominator in Eqn. (1) is an overall normalization constant which can be ignored if one is interested only in the relative merit of the various hypotheses. The term  $P(H)$  is our prior probability for the various models being compared. A uniform prior over all the models being considered would express our lack of inclination for any particular model. In this case the posterior probability  $P(H|D)$  in Eqn. 1, for the various hypotheses is proportional to the evidence.

### 2.2 Interpretation: what evidence measures

To gain a better intuitive understanding of evidence we now carry out the calculations analytically for a simple example. Assume that the likelihood  $P(D|\theta, H)$  is a Gaussian about the best fit likelihood position  $\theta_L$

$$P(D|\theta, H) = P(D|\theta_L, H) \exp \left[ -\frac{1}{2}(\theta - \theta_L)^T \mathbf{F}(\theta - \theta_L) \right] \quad (4)$$

where  $\mathbf{F}$  is the usual Fisher (curvature) matrix defined by  $F_{ij} = -\partial^2 [\log P(D|\theta, H)] / \partial\theta_i \partial\theta_j$  evaluated at  $\theta = \theta_L$ . Assume that the prior is also a Gaussian, but centred on  $\theta_P$  with curvature matrix  $\mathbf{P}$ . Evaluating the integral in Eq. 3 we find

<sup>1</sup> See at: <http://snap.lbl.gov>

<sup>2</sup> See at: <http://www.ctio.noao.edu/wproject>

<sup>3</sup> See at: <http://www.cfht.hawaii.edu>

$$\mathcal{E} = P(D|\boldsymbol{\theta}_L, H) \exp(-C) \left( \frac{|\mathbf{F} + \mathbf{P}|}{|\mathbf{P}|} \right)^{-1/2}, \quad (5)$$

where  $C$  is a constant depending on the degree of overlap between the prior and likelihood distributions. For the simpler case where  $\boldsymbol{\theta}_L = \boldsymbol{\theta}_P$  we find that  $C = 0$  and if we define volume under the prior  $V_{\text{prior}} = |\mathbf{P}|^{-1/2}$  and the volume under the posterior  $V_{\text{post}} = |\mathbf{F} + \mathbf{P}|^{-1/2}$  then the evidence becomes

$$\mathcal{E} \approx P(D|\boldsymbol{\theta}_0, H) \frac{V_{\text{post}}}{V_{\text{prior}}}. \quad (6)$$

The first term gives the usual likelihood at the best fit point, and the second fraction is the ratio between the volume under the posterior to the volume under the prior. Therefore evidence takes into account the likelihood at the best fit point, which usually increases with the number of parameters. However this is partially countered by the second term — the so called Occam's razor term — which ensures that models with a large number of parameters are penalised.

### 3 SUPERNOVAE

Type Ia supernova appear to be an excellent standard candle (Perlmutter et al. 1997; Riess et al. 1998), with a small dispersion in apparent magnitude,  $\sigma_{\text{mag}} = 0.15$ , with no evidence for evolution with redshift. The apparent magnitude is related to the luminosity distance through

$$m(z) = \mathcal{M} + 5 \log D_L(z) \quad (7)$$

where  $\mathcal{M} = M_0 + 5 \log [(c/H_0)/\text{Mpc}] + 25$ . The quantity  $M_0$  is the absolute magnitude of Type Ia SNe and  $D_L(z) = d_L(z)/(c/H_0)$  is the Hubble constant free luminosity distance. The combination of the absolute magnitude and the Hubble constant,  $\mathcal{M}$ , can be calibrated by low redshift supernovae, for instance the Calan/Tololo sample (Hamuy et al. 1993; Perlmutter et al. 1999). The dispersion in the magnitude,  $\sigma_{\text{mag}}$ , is related to the uncertainty in the inferred distance,  $\sigma$  by

$$\frac{\sigma}{d_L(z)} = \frac{\ln 10}{5} \sigma_{\text{mag}}. \quad (8)$$

This is about 7% for  $\sigma_{\text{mag}} = 0.15$ . In our simulations we assume that the errors in the luminosity distance are Gaussian. We neglect systematic errors in our calculations.

The SuperNova Acceleration Probe (SNAP) survey is expected to observe about 2000 Type Ia supernovae up to a redshift  $z \sim 1.7$ , each year (Aldering et al. 2002). Although the expected distribution of SNe is complicated, for our calculations we assume them to be uniformly distributed. Since a single supernova measures the luminosity distance with a relative error of  $\sim 7\%$ , binning the supernovae in  $\sim 50$  bins would give a relative error in the luminosity distance of about  $\sim 1\%$ .

For our simulations we calculate the luminosity distance in 50 redshift intervals up to a maximum redshift  $z = 1.7$ . We assume a relative error of 1% in the luminosity distance. Note that we *do not* add noise to the simulated distances. Therefore, our results only give the ensemble average of the various quantities that we quote below.

To decide which polynomial order is best suited to the data we now apply the notion of evidence. To label different

models we choose the letter  $N$  — the order of the polynomial approximation. The case of cosmological constant is denoted as  $N = -1$ . The only free parameters are the matter density  $\Omega_m$  and the polynomial coefficients  $\mathbf{w} = (w_i)$ . In reality we also have to marginalize over  $\mathcal{M}$ , but for simplicity we ignore this in our calculations. Therefore, our free parameters are  $\boldsymbol{\theta} = (\Omega_m, \mathbf{w})$ .

The likelihood function  $P(D|\boldsymbol{\theta}, N)$  is given by

$$P(D|\boldsymbol{\theta}, N) = \mathcal{N} \prod_{i=1}^{N_{\text{dat}}} \exp \left[ -\frac{1}{2} \left( \frac{d_L^{\text{fit}}(z_i, \boldsymbol{\theta}) - d_L(z_i)}{\sigma_i} \right)^2 \right], \quad (9)$$

where the index  $i$  ranges from 1 to  $N_{\text{dat}}$ , the number of supernovae in our sample (or the number of bins in redshift). The data is described by the measured luminosity distance  $d_L(z_i)$ , the dispersion  $\sigma_i$  and the redshift  $z_i$ . Also

$$d_L^{\text{fit}}(z) = \frac{c(1+z)}{H_0} \times \int_0^z \frac{(1+z')^{-3/2} dz'}{\sqrt{\Omega_m + \Omega_Q \exp \left\{ 3 \int_0^{z'} w(z'')/(1+z'') dz'' \right\}}}, \quad (10)$$

where  $w(z) = \sum_{i=0}^N w_i z^i$ ,  $\Omega_m$  is the present day fractional energy density in pressure-less matter and  $\Omega_Q = 1 - \Omega_m$  is the present day fractional density in dark energy. In Eqn. 9 the normalization constant  $\mathcal{N} = (2\pi)^{-N_{\text{dat}}/2} / \prod_{i=1}^{N_{\text{dat}}} \sigma_i$ .

## 4 EVIDENCE ANALYSIS

We begin this section by comparing evidence values for different theoretical models fitted to the current supernova data. We then repeat this exercise by simulating future data for various assumed input models and show how well evidence picks out the correct model. We then investigate the issues related to the effect of uncertainty in the matter density, and the effect of different priors on the dark energy parameters.

### 4.1 Current supernova data

Although the quality of data will continue to improve, it is instructive to see what the current supernova data tells us about which model to trust. For the analysis we use the compilation of supernova luminosity distances and redshifts by Tonry et al. (2003). We apply a prior of  $\Omega_m = 0.3 \pm 0.05$  (similar to Allen, Schmidt & Fabian 2002). In Fig. 1 we plot the 68% and 95% contours. As expected the error bars are large. The peak of the likelihood surface lies in the region where  $w < -1$ . Table 4.1 gives the computed evidence values for various models with two different priors for  $w(z)$ : the first row gives the evidence values with the prior  $-1.5 \leq w_0 \leq 0$ ,  $-2 \leq w_1 \leq 1$  (limits of Figure 1), and the second row gives evidence with the prior  $-1 \leq w(z) \leq 1$ , in the range  $0 \leq z \leq 1.7$ . As expected from Figure 1 the simplest  $\Lambda$  model has the largest evidence with either prior. The data favours the simplest model but still allows the possibility of some evolution in agreement with the contours plotted in Fig. 1. Since the peak of the posterior does not lie in the region given by the second prior  $-1 \leq w(z) \leq 1$ , we find that with

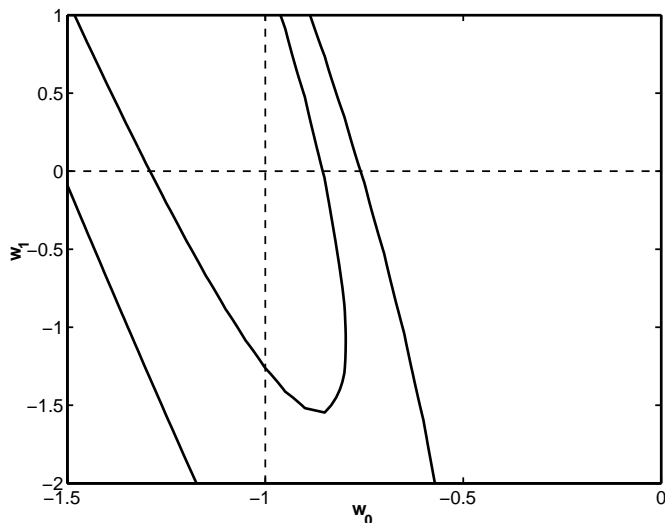


**Figure 1.** The 68% and 95% joint likelihood contours for  $w_0 - w_1$  with current Supernova data (Tonry et al. 2003), marginalized over  $\Omega_m$  with a Gaussian prior,  $\Omega_m = 0.3 \pm 0.05$ , and a uniform prior for the equation of state in the range  $-1.5 \leq w_0 \leq 0$  and  $-2.0 \leq w_1 \leq 1.0$ .

Prior	$w = -1$	$w = w_0$	$w = w_0 + w_1 z$
$-1.5 \leq w_0 \leq 1$	66.6%	18.1%	15.3%
$-2 \leq w_1 \leq 1$			
$-1 \leq w(z) \leq 1$	91.0%	6.0%	3.0%

**Table 1.** Evidence for the Supernova luminosity distances given in Tonry et al. (2003). We have used the tight prior  $\Omega_m = 0.3 \pm 0.05$  for this calculation.

this prior the data is more consistent with the cosmological constant.

## 4.2 The discriminatory power of future supernova surveys

We simulate luminosity distance for a SNAP like experiment as described in Section 3. First we consider a linearly evolving equation of state given by  $w(z) = -0.8 + 0.6z$  with  $\Omega_m = 0.3$ . This choice of parameters illustrates certain degeneracies first described in Maor et al. (2002) In Fig 2 we plot the 68% confidence contours in the  $w_0 - w_1$  plane, marginalized over  $\Omega_m$ , for different priors on  $\Omega_m$ . For the dark energy we chose the priors  $-1.5 \leq w_0 \leq 0$  and  $-2 \leq w_1 \leq 1$  in this calculation. We address the issue of priors on the dark energy in detail in Section 4.4. We see how the joint likelihood contours tighten as  $\Omega_m$  is increasingly constrained.

We also plot contours using a Gaussian approximation to the peak of the posterior for a prior  $0 \leq \Omega_m \leq 1$ . Comparing with the corresponding exact calculation shows that the Fisher matrix error bars are very misleading. This is not surprising since Fisher matrix only gives the minimum variance for the extracted parameters. The correct contours also show that the distribution of the equation of state param-

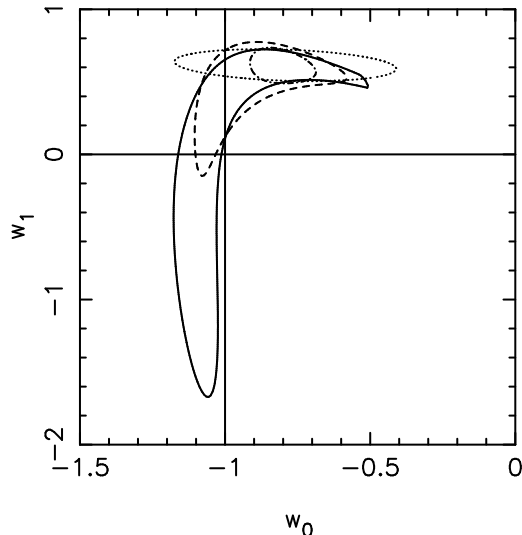


**Figure 2.** The marginalized 68% joint likelihood contours in the  $w_0 - w_1$  plane for an input model  $w(z) = -0.8 + 0.6z$  and  $\Omega_m = 0.3$  for various priors on  $\Omega_m$ . The solid line is for a flat prior in the range  $0 < \Omega_m < 1$ , the dashed line a Gaussian prior with  $\Omega_m = 0.3 \pm 0.1$  and the dot-dashed line a Gaussian prior with  $\Omega_m = 0.3 \pm 0.05$ . The dotted line is the result of a Fisher matrix analysis.

eters  $w_0$  and  $w_1$  is not close to Gaussian. Therefore, for our calculations below we do not use Fisher matrix approximations described in Sec. 2.2.

We now investigate how well the evidence can infer the required polynomial order for the equation of state. For this purpose we choose to consider fitting models only up to a linear order, including the case of a cosmological constant model ( $\Lambda$  model). Therefore, our model space comprises (1) the  $\Lambda$  model with  $w(z) = -1$ ; (2) the constant equation of state model with  $w(z) = w_0$  and (3) the linearly evolving model with  $w(z) = w_0 + w_1 z$ . In Figure 3 we plot the normalized probabilities as a function of fitting models, for various input models. For this figure we assumed a tight prior on  $\Omega_m = 0.3 \pm 0.05$ . Evidence clearly picks out the correct polynomial order for the  $\Lambda$  model (solid line), the model with  $w(z) = -0.7$  (short dashed line) the model with  $w(z) = -0.8 + 0.6z$  (dotted line). Here we have also considered a model with a weaker redshift evolution,  $w(z) = -0.8 + 0.3z$  (long-dashed line). We find that for this case the evidence marginally prefers a model with no redshift evolution, although the evidence is very similar for all three models. The evolution in the equation of state in this model is clearly not sufficient to be established by SNAP. In general the evidence tends to be conservative in this respect and favours simpler models.

## 4.3 Effect of uncertainty in $\Omega_m$

The greatest uncertainty in constraining  $w(z)$  comes from the fact that the value of  $\Omega_m$  is not very well known. To illustrate the effect of choosing different priors for  $\Omega_m$  we calculate the evidence for model  $w(z) = -0.8 + 0.6z$  with the following three priors on  $\Omega_m$ : (1) A uniform prior in the range  $0 < \Omega_m < 1$ , (2) a Gaussian prior with  $\sigma_{\Omega_m} = 0.1$  and (3) a Gaussian prior with  $\sigma_{\Omega_m} = 0.05$ . Our results are

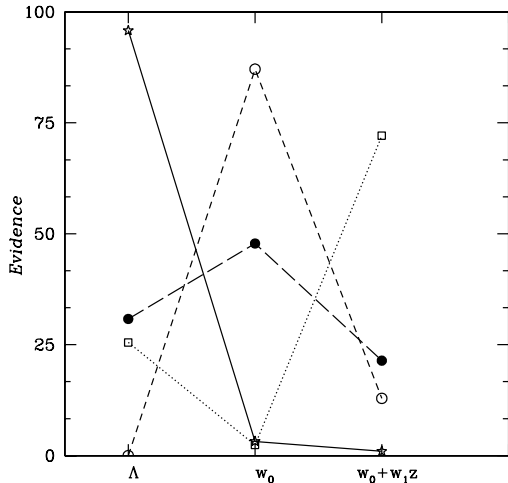


**Figure 3.** Evidence values (in percent) for various models, and various levels of fit as indicated on the x-axis, with a Gaussian prior  $\Omega_m = 0.3 \pm 0.05$ . The solid line is for an input  $\Lambda$  model, the short dashed line for an input model with  $w(z) = -0.7$ , the long-dashed line for a model with  $w(z) = -0.8 + 0.3z$  and the dotted line for  $w(z) = -0.8 + 0.6z$ .

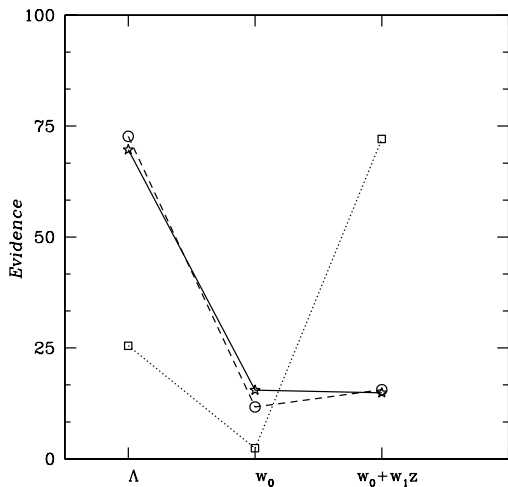


**Figure 4.** Evidence values for the model  $w(z) = -0.8 + 0.6z$  with various levels of fit as indicated on the x-axis. The solid line is for a uniform prior in the range  $0 < \Omega_m < 1$ , the dashed line for a Gaussian prior,  $\Omega_m = 0.3 \pm 0.1$  and the dotted line as in Fig. 3 a prior of  $\Omega_m = 0.3 \pm 0.05$ .

plotted in Fig. 4. The correct model is picked out only in the case where the prior on the matter density is the tightest,  $\sigma_{\Omega_m} = 0.05$ .

The real difficulty is the degeneracy that exists between a fast evolving model and a cosmological constant model with an incorrect value of  $\Omega_m$  (Maor et al. 2002). This can be understood from Fig. 5, where we plot the log-evidence for the three models as a function of assumed values of  $\Omega_m$ . We see that the evidence for the true linear model is nearly constant and stays above the evidence for the other two models until  $\Omega_m \sim 0.46$ , where a degenerate case appears

which fits best to the cosmological constant model, and the worst to the linear model. In fact, the  $\Lambda$  model with  $\Omega_m = 0.46$  and the linear model with the correct  $\Omega_m$  have nearly the same likelihood, so the evidence decides on the basis of the Occam’s razor term and penalises the more complex model. As a result the uniform prior of  $0 < \Omega_m < 1$  prefers the  $\Lambda$  model, and since the Gaussian prior with  $\Omega_m = 0.3 \pm 0.1$  model does not rule out  $\Omega_m = 0.46$  sufficiently strongly, it still assigns the largest probability to the  $\Lambda$  model. In fact the correct inference is drawn if either the priors on  $\Omega_m$  are tight, or if we have a hard upper bound at  $\Omega_m \sim 0.4$ , as Fig. 5 clearly demonstrates.

This result can also be understood in terms of Fig. 2. The cosmological constant model corresponds to the intersection of the axes at  $w_0 = -1$ ,  $w_1 = 0$ . For the two widest  $\Omega_m$  priors the 68 per cent contours almost include the cosmological constant model, which explains why evidence uses Occam’s razor to pick this model. Whereas for the tightest prior on  $\Omega_m$  the 68 per cent confidence contours are far from the cosmological constant model, and indeed, as expected, the integrated probability (evidence) disfavours it.

Constraints on  $\Omega_m$  can be obtained by including other cosmological measurements with the supernova data. Some probes such as the CMB and cosmic shear (see Refregier et al, 2003) are sensitive to a combination of  $w$  and  $\Omega_m$ , so this must be taken into account. In addition care must be taken since the CMB probes the equation of state at a higher mean redshift and so may have a different effective constant equation of state (eg. Saini et al. 2003) and is sensitive to perturbations. On the other hand there are some local measures that are largely insensitive to  $w$  or its evolution, such as the baryon fraction in clusters and mass-to-light ratios (Bahcall et al. 2000). A recent analysis of the baryon fraction in clusters using Chandra data (Allen, Schmidt & Fabian 2002) puts a ten per cent uncertainty on the matter density when HST key project and nucleosynthesis information is used.

#### 4.4 Effect of priors on $w$

The evidence is affected by the assumed choice of priors on the parameter values. Qualitatively, increasing the width of the priors on  $w$  will increasingly disfavour models with more parameters, which is clearly seen in Eqn. 6. The priors in the previous section were arbitrarily chosen to be consistent with the input models and to have enough room for a fair degree of uncertainty prior to the data. We also note that although in principle one could imagine physical reasons for limiting  $w_0$  within a certain range, the dimensional quantity  $w_1 = dw/dz$  could in principle be arbitrarily large. Therefore, a better, physically motivated prior is not on the polynomial coefficients but on the  $w(z)$  itself. For a subclass of dark energy models the equation of state satisfies the constraint  $-1 \leq w(z) \leq 1$ . Figure 6 shows the effect of choosing this prior. We find that the evidence is better able to pick the correct model in this case relative to the choice of priors in the last section. For this subclass of theoretical models the prospects for disentangling the dark energy properties are seen to be much better.

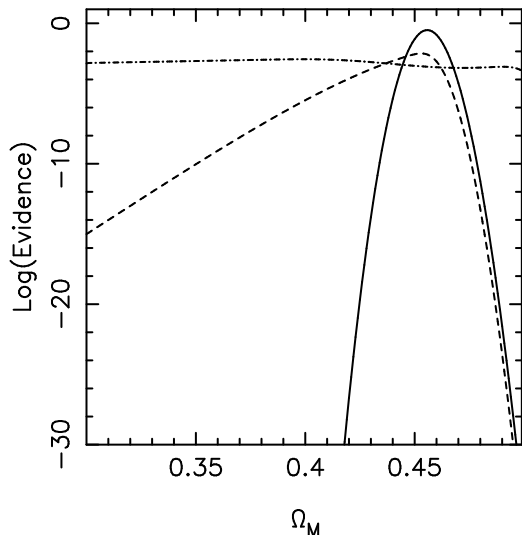


**Figure 5.** Log of evidence plotted for the input model  $w_0 = -0.8$  and  $w_1 = 0.6$  with  $\Omega_m = 0.3$  as a function of  $\Omega_m$  assumed for the fit. The solid line corresponds to the fit to a cosmological constant, the dashed line corresponds to the fit to a constant  $w$  and the dot-dashed line corresponds to the linear fit respectively. It should be noted that the evidence is left un-normalized.

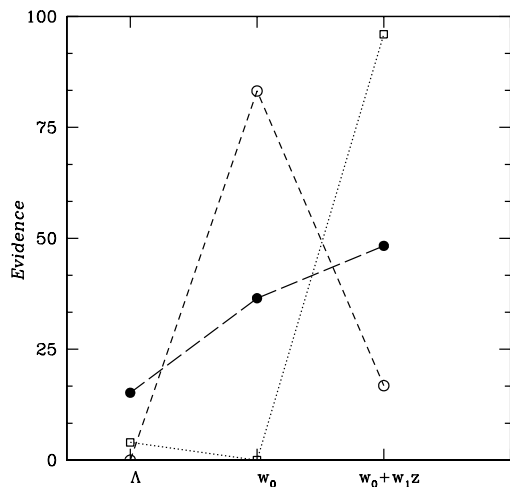


**Figure 6.** Evidence values for various models, and various levels of fit as indicated on the x-axis, with a Gaussian prior  $\Omega_m = 0.3 \pm 0.05$ , and a uniform prior on the equation of state in the range  $-1 \leq w(z) \leq 1$ . The dotted line is for an input model with  $w(z) = -0.8 + 0.6z$ , the short dashed line for an input model with  $w(z) = -0.7$ , the long-dashed line for a model with  $w(z) = -0.8 + 0.3z$ .

## 5 CONCLUSIONS

We have investigated the use of Bayesian evidence for establishing the significance of fitting cosmological data to various models of the dark energy. By focusing on a polynomial approximation for the unknown equation of state parameter  $w(z)$  we have shown how evidence can be used to fix the polynomial order, thereby establishing the minimum variation in  $w(z)$  required to fit the data adequately.

We find that the evidence is affected by the priors. The

largest uncertainty in establishing the nature of dark energy stems from the lack of knowledge of the precise value of the present day density in the form of pressureless dark matter. Our results for the currently available SNe show that the current data favours the simplest case of cosmological constant. Since the peak of the likelihood lies in the range  $w_0 < -1$ , the tight prior  $-1 \leq w(z) \leq 1$  disfavors the more complex models more strongly.

We have shown that for a SNAP like data set, if one uses “wide” priors on the polynomial coefficients, evidence will enable us to decide if the data is best fit to a model with a cosmological constant, by a constant equation of state or, if the evolution is larger than  $w_1 \sim 0.5$ , to a linear model. We have shown that our conclusions can be significantly improved if we narrow the range of dark energy parameters by employing a prior of the form  $-1 \leq w(z) \leq 1$ , which happens naturally for a subclass of dark energy models. This prior establishes the correct order of polynomial even for relatively modest evolution in the equation of state. However, since there are models which allow, albeit in a contrived way,  $w < -1$ , we have allowed for these models in our examples.

To summarize, we have shown that evidence can be a powerful tool for systematically pinning down the nature of dark energy. Its application to the polynomial approximation for the equation of state parameter allows us to fix the polynomial order that is required by data. The simple relation between the polynomial coefficients and the underlying true equation of state enables us to obtain all the properties of dark energy provided by the data.

## 6 ACKNOWLEDGEMENT

We thank Rob Crittenden, Steve Gull, David MacKay, Phil Marshall, Thanu Padmanabhan and Ben Wandelt for helpful discussions. TDS thanks PPARC for financial support. SLB acknowledges support from a Selwyn College Trevelyan Research Fellowship. JW is supported by the Leverhulme Trust and a Kings College Trapnell Fellowship.

## REFERENCES

- Aldering, G. and the SNAP collaboration, 2002, SPIE, 4835, to appear.
- Allen, S.W. , Schmidt, R.W. , Fabian, A. C., 2002, astro-ph/0205007.
- Amendola, L., 2000, Phys. Rev., D62, 043511.
- Armendariz-Picon, C., Mukhanov, V., Steinhardt, P. J., 2000, Phys. Rev. Lett., 85, 4438.
- Bahcall, N., Cen, R., Davé, R., Ostriker, J., Q. Yu, 2000, Ap. J., 541, , 1
- Bahcall, N. , Fan, X., 1998, Ap. J., 504, 1.
- Balbi, A. et al. , 2000, Ap. J. Lett., 545, 1.
- Bean, R. , Melchiorri, A., 2002, Phys. Rev., D65, 041302.
- de Bernadis, P. et al. , 2000, Nature, 404, 955.
- de Bernadis, P. et al. , 2002, Ap. J., 564, 559.
- Carroll, S.M., 2001, Living Rev. Rel., 4, 1.
- Chiba, T., 1999, 1999, Phys. Rev., D60.083508
- Dodelson, S. , Knox, L., 2000, Phys. Rev. Lett., 84, 3523.
- Efstathiou, G., 1999, MNRAS, 310, 842.
- Efstathiou, G. et al. , 2002, MNRAS, 330, L29.
- Garnavich, P.M. et al. , 1998, Ap. J., 509, 74.
- Garnavich, P.M. et al. , 2003, 2003, BAAS, 201.7809

- Gerke, B.F. , Efstathiou, G., 2002, astro-ph/0201336.
- Goliath, M. et al. , 2001, Astron. Ap., 380, 6.
- Halverson, N.W. et al. , 2002, Ap. J., 568, 38.
- Hamuy, M. et al. , 1993, Ap. J., 106, 2392.
- Hanany, S. et al. , 2000, Ap. J. Lett., 545, 5.
- Lange, A.E. et al. , 2001, Phys. Rev., D63, 042001.
- Lewis, A. & Bridle, S., 2002, astro-ph/0205436.
- MacKay, D.J.C. 1991, Neural Computation
- Maor, I. ,Brustein, R. , Steinhardt, P.J., 2001, Phys. Rev. Lett., 86, 6.
- Maor, I. et al. , 2002, Phys. Rev., D65, 123003.
- Mohr, J.J. , Mathiesen, B. , Evrard, A. .E, 1999, Ap. J., 517, 627.
- Netterfield, C.B. et al. , 2002, Ap. J., 571, 604.
- Peebles, P.J.E. , Ratra, B., 1988, Ap. J., 325, L17.
- Percival, W. et al. , 2002, astro-ph/0206256.
- Perlmutter, S. et al. , 1997, Ap. J., 483, 565.
- Perlmutter, S. et al. , 1999, Ap. J., 517, 565.
- Perlmutter, S. , Turner, S. , White, M., 1999, Phys. Rev. Lett., 83, 670.
- Pryke, C. et al. , 2002, Ap. J., 568, 46.
- Ratra, B. , Peebles, P.J.E., 1988, Phys. Rev., D37, 3406.
- Refregier, A. et al. , 2003, astro-ph/0304419.
- Riess, A.et al. , 1998, Astron. J, 116, 1009.
- Riess, A.et al. , 2001, Ap. J., 560, 49.
- Rubino-Martin, J.A. et al. , 2002, astro-ph/0205367.
- Sahni, V. et al. , 2002, astro-ph/0201498.
- Saini. T.D., Padamanbhan, T., Bridle, S., 2003, astro-ph/0301536.
- Sievers, J.L. et al. , 2002, astro-ph/0205387.
- Sivia D.S. , 1996, *Data Analysis: A Bayesian Tutorial*. Oxford University Press
- Spergel, D.N. et al. , 2003, astro-ph/0302209.
- Tonry, J.L. et al. , 2003, astro-ph/0305008.
- Hinshaw, G. et al. , 2003, astro-ph/0302217.
- Steinhardt, P.J. , Wang, L. , Zlatev, I., 1999, Phys. Rev., D 59, 123504.
- Stompor, R. et al. , 2001, Ap. J. Lett., 561, 7.
- Uzan, J.P., 1999, Phys. Rev., D59, 123510.
- Weinberg, S., 1989, Rev. Mod. Phys., 61, 1.
- Weller, J. , Albrecht, A., 2001, Phys. Rev. Lett., 86, 1939.
- Weller, J. , Albrecht, A., 2002, Phys. Rev., D65, 103512.
- Wetterich, C., 1988, Nucl. Phys., B302, 668.
- Zel'dovich, Ya.B., 1968, Sov. Phys. Usp., 11, 381.